Relaxation Dynamics of Hydrated Thymine, Thymidine, and Thymidine Monophosphate Probed by Liquid Jet Time-Resolved Photoelectron Spectroscopy

Blake A. Erickson,[†] Zachary N. Heim,[†] Elisa Pieri,[‡] Erica Liu,[†] Todd J. Martinez,[‡] and Daniel M. Neumark*[,†,§]

[†]Department of Chemistry, University of California, Berkeley, California 94720, United States

[‡]Department of Chemistry, Stanford University, Stanford, California 94305, United States

[§]Chemical Sciences Division, Lawrence Berkeley National Laboratory, Berkeley, California 94720, United States

ABSTRACT: The relaxation dynamics of thymine and its derivatives thymidine and thymidine monophosphate are studied using time-resolved photoelectron spectroscopy applied to a water microjet. Two absorption bands are studied; the first is a bright $\pi\pi^*$ state which is populated using tunable-ultraviolet light in the range 4.74−5.17 eV and probed using a 6.20 eV probe pulse. By reversing the order of these pulses, a band containing multiple $\pi\pi^*$ states is populated by the 6.20 eV pulse and the lower energy pulse serves as the probe. The lower lying $\pi\pi^*$ state is found to decay in ∼400 fs in both thymine and thymidine independent of pump photon energy, while thymidine monophosphate decays vary from 670 to 840 fs with some pump energy dependence. The application of a computational quantum mechanical/molecular mechanical scheme at the XMS-CASPT2//CASSCF/AMBER level of theory suggests that conformational differences existing between thymidine and thymidine monophosphate in solution account for this difference. The higher lying $\pi\pi^*$ band is found to decay in ∼600 fs in all three cases, but it is only able to be characterized when the 5.17 eV probe pulse is used. Notably, no long-lived signal from an $n\pi^*$ state can be identified in either experiment on any of the three molecules.

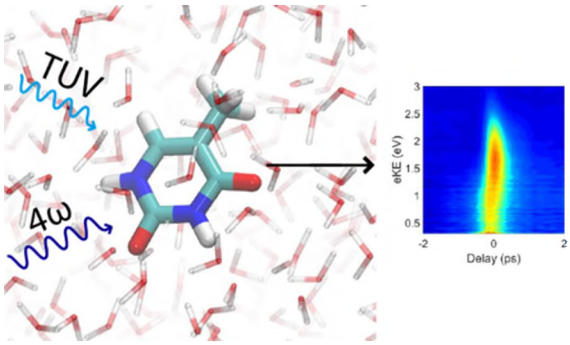

■ INTRODUCTION

DNA strongly absorbs ultraviolet (UV) light, but shows very small rates of damage subsequent to this absorption.[1−5] Understanding the mechanism by which DNA disposes of this excess energy is a crucial element of photobiology. Because of the complexity of DNA strands, many laboratories have undertaken a "bottom-up" approach to the elucidation of these dynamics by investigating smaller nucleic acid (NA) constituents such as nucleobases, nucleosides, and nucleotides.[6] While many of these studies have been performed on isolated gas phase molecules,[7] the ability of NA constituents to dissipate excess energy into the surrounding solvent environment (namely, water) is of particular interest.[8] To this end, we have investigated the relaxation dynamics of aqueous thymine (T), thymidine (Thd), and thymidine monophosphate (TMP) by time-resolved photoelectron spectroscopy (TRPES) of liquid water microjets, focusing on excitation of absorption bands at 4.74−5.17 and 6.20 eV.

T and its derivatives show strong absorption features at ∼265 and ∼205 nm (4.68 and 6.05 eV) in water.[9−11] These bands exhibit little change going from the nucleobase to the nucleotide, indicating these excitations are likely localized to the nucleobase itself.[12] The assignment of the absorption spectrum has been considered in numerous studies on the electronic structure of thymine[13−16] that are well-reviewed by Improta et al.[5] This body of work shows that, in isolated T, the lower energy absorption band corresponds to a $\pi\pi^*$ highest occupied molecular orbital (HOMO) → lowest unoccupied molecular orbital (LUMO) transition while the optically dark $n\pi^*$ (HOMO − 1) → LUMO transition lies lower in energy. In water, the $\pi\pi^*$ state is stabilized while the $n\pi^*$ state is destabilized,[17] causing the $\pi\pi^*$ and $n\pi^*$ states to be near-degenerate. The higher lying absorption band at ∼205 nm also appears to be of $\pi\pi^*$ character based on comparison to gas phase results,[5] and recent calculations indicate that multiple $\pi\pi^*$ transitions contribute to this band in liquid water.[11] For convenience, the ground state will be referred to as S_0 and the higher lying band will be referred to as S_n to distinguish it from the lower lying $\pi\pi^*$ state.

Photodeactivation of the first $\pi\pi^*$ state has been studied in T in the gas phase using time-resolved photoionization,[18−20] photoelectron spectroscopy (TRPES),[21,22] and X-ray transient

absorption.[23] These experiments find a subpicosecond decay component that is most often attributed to relaxation through a conical intersection (CI) connecting the initially populated $\pi\pi^*$ state and the lower energy $n\pi^*$ state. A recent TRPES experiment using an extreme ultraviolet (XUV) probe energy[24] has found that the population in the $n\pi^*$ state is then transferred to a $^3\pi\pi^*$ state in a few picoseconds, although there is still some contention on this point. Theoretical investigations largely agree on this mechanistic picture of relaxation for isolated T.[22,25,26]

Since the relative energies of the states change upon solvation such that the $n\pi^*$ state is similar to or higher in energy than the $\pi\pi^*$ state, it remains to be seen whether this state is still involved in the relaxation process when solvated. The relaxation mechanism of T and, in some cases, Thd and TMP, have been studied in liquid water by fluorescence upconversion (FU),[27,28] ultraviolet/visible and infrared transient absorption (TA),[29−33] and TRPES.[34] FU studies have fit the decays of all three species to a single lifetime attributed to direct relaxation from $\pi\pi^* \rightarrow S_0$. In contrast, the TA studies generally find two decay lifetimes: a subpicosecond decay that corresponds to direct repopulation of the ground state, and an additional multiple picosecond decay that has most often been attributed to the $n\pi^*$ state. A bifurcation is seen in the signal with the majority directly going from $\pi\pi^* \rightarrow S_0$, with the remainder proposed to be relaxing by $\pi\pi^* \rightarrow n\pi^* \rightarrow S_0$. Although this discrepancy is far from settled, a recent calculation suggests that population transfer from $\pi\pi^* \rightarrow n\pi^*$ is significantly weaker in water than in isolated T and changes drastically with small changes in the energy gap between the two states.[35]

The relaxation dynamics of nucleic acid constituents in aqueous solution have recently been addressed in a series of TRPES experiments on liquid water microjets.[34,36−38] These jets enable the study of bulk aqueous solutions under vacuum using single photon[39,40] and time-resolved[41,42] photoelectron spectroscopies, techniques that were previously restricted to gas-phase studies. Lübcke and co-workers[34] have carried out liquid jet TRPES on T and Thd. They find biexponential decay on two subpicosecond time scales and attribute both of these decay channels to $\pi\pi^* \rightarrow S_0$ direct relaxation along different pathways on the $\pi\pi^*$ surface. Notably, no long-lived signal was seen, which could indicate the absence of the $n\pi^*$ state being on the decay pathway or insufficient probe energy to photoionize the state. Calculations in that work suggested that the probe energy (5.20 eV) should have been high enough to see photoemission from the $n\pi^*$ state, but there are other excited states, such as the $^3\pi\pi^*$ state, that have binding energies greater than 5.20 eV that would not be visible to their experiment.[17]

In this work, TMP is studied by liquid microjet TRPES for the first time, along with T and Thd. A higher probe energy of 6.20 eV is used, compared to previous liquid jet work on T and Thd where the maximum probe energy was 5.20 eV.[34] As will be discussed, this ensures that ionization from all singlet excited states is energetically accessible and provides more insight into the possible role of the $n\pi^*$ state in the relaxation of T, Thd, and TMP. Finally, relaxation from the second absorption band at 6.20 eV is studied for the first time in all three molecules by reversing the pump pulse and the probe pulse, showing new decay pathways along multiple excited state surfaces for the first time. Interpretation of the results, particularly differences between TMP and the other two molecules, is aided by molecular dynamics simulations.

METHODS

The apparatus used in these experiments has been described in detail previously.[38,43−47] Briefly, two femtosecond laser pulses cross a liquid water microjet in which the species of interest is dissolved. Photoelectrons ejected from the jet are analyzed using a magnetic bottle time-of-flight (ToF) analyzer. The overall experiment is summarized as follows:

$$T \xrightarrow{h\nu_1} T^* \xrightarrow{\Delta t, h\nu_2} T^+ + e^-(eKE) \quad (1)$$

In the positive delay direction, a tunable UV pump pulse (4.74−5.17 eV), $h\nu_1$, electronically excites the nucleic acid constituent and a 6.20 eV probe pulse, $h\nu_2$, photoionizes the excited species. A variable delay time Δt is applied between the two pulses which allows the collection of time-resolved data. In the negative delay direction, the 6.20 eV pulse arrives first and the tunable UV serves as the probe. Thymine (Sigma-Aldrich, 10 mM), thymidine (United States Biochemical Corp., 10 mM), and thymidine monophosphate (Sigma-Aldrich, 7 mM) were dissolved in water buffered at pH 8 with Trizma HCl (2 mM, Sigma-Aldrich), and NaCl (100 mM, Sigma-Aldrich) was added to reduce the streaming potential. These samples were introduced to a vacuum through a 20 μm capillary with a flow rate of 0.2 mL/min. At the point of probing, our jet is calculated to be ∼280 K based on Faubel's evaporative cooling model for liquid microjets.[48] The solutions of Trizma HCl and NaCl provided no time-resolved signal as is shown in Figure S4 in the Supporting Information.

A Ti:sapphire laser (Coherent Astrella) generated 35 fs, 7 mJ pulses centered at 800 nm at a 1 kHz repetition rate. Approximately 1 mJ of this beam was directed into a Light Conversion TOPAS-Prime optical parametric amplifier with an NIRUVis extension to generate the tunable UV pulses (4.74−5.17 eV). Also, 1 mJ was sent into a β-barium borate (BBO) based sum frequency generation line to generate the fourth harmonic of the fundamental laser output (6.20 eV). The energy of each pulse was set between 20 and 50 nJ as measured directly before entering the liquid jet vacuum chamber. The pulse durations were measured as a cross-correlation, or instrument response function (IRF), between the two pulses that was found to be ∼160 fs by 2 + 1 resonantly enhanced multiphoton ionization of Xe using 5.00 and 6.20 eV pulses, respectively. The actual IRF for each experiment was fit with the data as it was found to change daily and with tunable UV energy. The cross-correlation is dependent on the photon energy produced by the optical parametric amplifier as no compression is done after generation. The tunable UV light passed through a delay stage (Newport, ILS150PP) that was variably delayed from the other pulse from −3.0 to 4.5 ps. Scans were performed taking 1000 shots at each delay before moving the stage and static two-photon, one-color backgrounds were taken after each scan of delays with the stage set to a 0 ps delay.

The ejected photoelectrons were directed into the magnetic bottle ToF spectrometer through a 900 μm diameter skimmer located 1 mm from the jet by a 1.1 T rare earth magnet stack composed of SmCo/Nd disk magnets, and then guided through a 66 cm flight tube by an axial 10 G field from a solenoid. Photoelectrons were detected by a microchannel plate (MCP) stack with a phosphor screen. The arrival times of

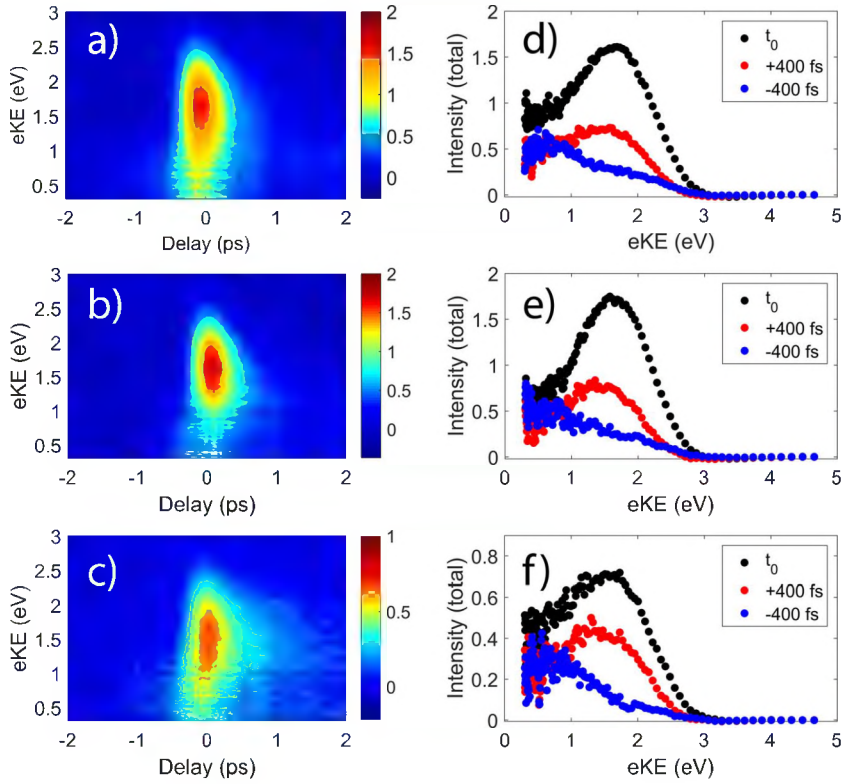

Figure 1. Processed data for 4.95/6.20 eV (positive delays) and 6.20/4.95 eV (negative delays) experiments. (a–c) Filled contour plots for T, Thd, and TMP. (d–f) Select lineouts to show the two features. Peak A is in red and peak B is in blue. The black trace shows when the two pulses are overlapped in time.

the electrons were recorded by capacitively coupling the current off of the back MCP as a function of time after the probe pulse hits the jet. The phosphor screen image was used for alignment of the magnetic bottle.

The spectrum measured at each delay was background subtracted from the one-color, two-photon spectra. The ToF distribution measured by the spectrometer was converted to electron kinetic energy (eKE). Global lifetime analysis (GLA) was used to fit the spectra and lifetimes using a minimum number of kinetic components.[46,49,50]

In brief, GLA can fit a time-resolved data set according to the following equation:

$$S(\mathrm{eKE}, \Delta t) = \sum_{i=1}^{n} \mathrm{DAS}_{\tau_i}(\mathrm{eKE})[\mathrm{e}^{-t/\tau_i} L(t - \Delta t)] \quad (2)$$

Equation 2 permits the determination of spectra and lifetimes of time-resolved data. Two assumptions are involved. (1) Spectral components shift only in intensity, not in energy. This allows the separability of the components dependent on eKE and the kinetics of the corresponding component which depend on pump–probe delay. (2) The kinetics can be expressed as a simple sum of monoexponential decays, thereby enabling data to be represented as a sum of exponentials and the IRF mentioned earlier, $L(t - \Delta t)$, multiplied by an energy dependent term called the decay associated spectrum (DAS_{τ_i}) and a time constant ($\tau_i = 1/k_i$).

Numerical simulations were performed to elucidate the mechanism behind the observed signals. For all three of the target species (T, Thd, TMP), we carried out 100 ns of molecular dynamics including the aqueous solvent at 300 K with the AMBER FF14SB and SPC force fields (see the Supporting Information for full details). For each of the three target species, a clustering analysis based on root-mean-square deviation of the solute was used to obtain the most likely solute geometries and to guide further sampling. We then extracted 1000 snapshots from each molecular dynamics trajectory, under the constraint that the relative population of different clusters followed that found in analysis of the 100 ns trajectory. Absorption spectra were calculated by histogramming the energy gaps obtained from these 1000 snapshots using quantum mechanics/molecular mechanics (QM/MM) with CASSCF(8/6) and the 6-31G* basis set for the solute and the SPC force field for surrounding water molecules. We further selected 100 snapshots for each molecule to compute the QM/MM absorption spectra with XMS-CASPT2(8/7) in the 6-31G* basis set for the solute. Details on the computational methods can be found in the Supporting Information.

■ RESULTS

Time-resolved photoelectron spectra of T, Thd, and TMP are presented in Figures 1a–c and 2a–c. The data presented were taken at pump photon energies of 4.95 and 5.17 eV, respectively, and a 6.20 eV probe photon energy. Results at 4.74 eV pump photon energy, which are quite similar to the spectra in Figure 1, are shown in Figure S1. The role of the pump and probe pulses is reversed at negative times, in which case the pump photon energy is 6.20 eV.

The spectra in Figure 1 are asymmetric with respect to t_0, showing decays in the positive delay direction and very little signal in the negative delay direction. All three of the spectra

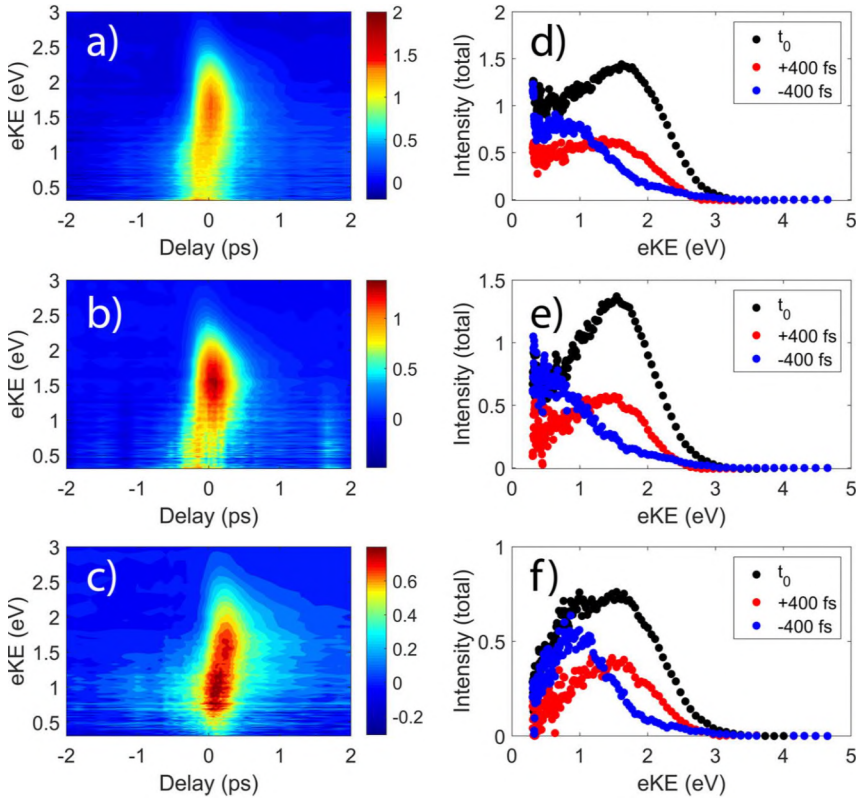

Figure 2. Processed data for 5.17/6.20 eV (positive delays) and 6.20/5.17 eV (negative delays) experiments. (a–c) Filled contour plots for T, Thd, and TMP. (d–f) Select lineouts to show the two features. Peak A is in red and peak B is in blue. The black trace shows when the two pulses are overlapped in time.

are peaked at eKE ~ 1.5 eV. For T and Thd, most of the signal decays completely within ~0.75 ps, while TMP shows a longer lived signal that persists until ~1.5 ps. The spectra of T, Thd, and TMP in Figure 2 are similar to those in Figure 1 for positive time delays but show significantly different behavior for negative time delays, with a signal peaked below 1 eV persisting beyond −0.5 ps. As in Figure 1, signal from TMP lasts noticeably longer compared to T or Thd; in Figure 2 this occurs in both the positive and negative directions.

To analyze these features further, spectral lineouts were taken at selected delays and are shown in Figures 1d–f and 2d–f. Lineouts were taken at t_0 (i.e., zero pump–probe delay) as well as at +400 and −400 fs, where any contributions from pump–probe overlap should be negligible. In the positive direction, there is a peak located at ~1.5 eV (referred to as peak A and shown in red) for all three species, whereas in the negative direction there is a peak located at ~0.8 eV (referred to as peak B and shown in blue). Peak B is stronger and persists much longer when probing at 5.17 eV compared to 4.95 eV, and is particularly noticeable for TMP at 5.17 eV. Select lineouts out to 4 ps for the 4.95/6.20 eV experiment on TMP are shown in Figure 3. These lineouts show the evolution of peak A in the long time limit.

The maxima in the eKE distributions for features A and B are ~1.5 and ~0.8 eV, respectively, and are the same for each of the three species studied. The vertical detachment energies (VDEs) of features A and B, calculated as the difference between the probe photon energy and the peak of the eKE distribution measured, are found to be ~4.7 and ~4.4 eV, respectively. These values are quite close, indicating that both

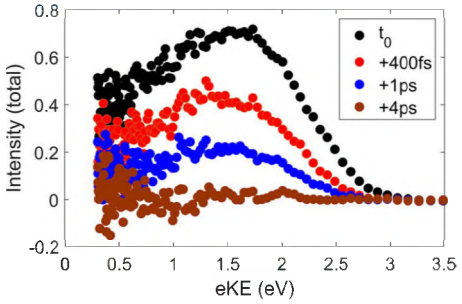

Figure 3. Select lineouts shown for the 4.95/6.20 eV experiment in TMP. The signal is found to decay completely within a few picoseconds with no emergence of a new signal at long times.

features reflect photodetachment from the same state: the lowest energy $\pi\pi^*$ state. Features A and B do not shift significantly on the time scale of the experiment, but they do overlap around t_0.

Because of the overlap, the results for T, Thd, and TMP were fit using the GLA routine described under Methods. The comparison between the GLA fit and the total integrated signal is shown in parts a and b of Figure 4 for TMP for 4.95 and 5.17 eV, respectively, plotted as a function of the delay. For 4.74/6.20 and 4.95/6.20 eV experiments, only one kinetic component in the positive direction was needed to fit the data. There is some signal that is not reproduced in the negative direction, but it is too weak to fit reliably. For the 5.17/6.20 eV experiments, two kinetic components were

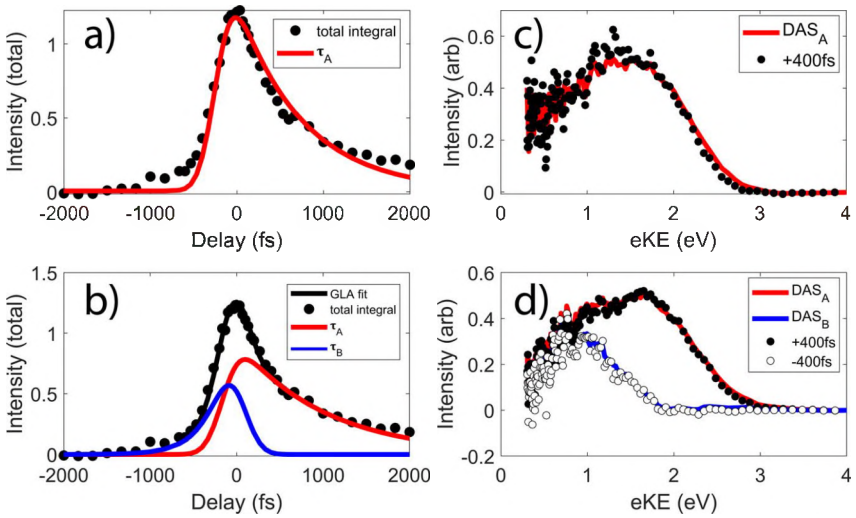

Figure 4. (a, b) Comparison between the GLA fits for the 4.95/6.20 and 5.17/6.20 eV experiments for TMP, respectively. In the 4.95/6.20 eV experiment only one decay is found in the positive direction, while two decays are found in the 5.17/6.20 eV experiment. (c, d) Comparison between the DAS and lineouts at +400 fs in the 4.95/6.20 eV experiment and ±400 fs in the 5.17/6.20 eV experiments.

required to fit the data, one in the positive delay direction and one in the negative delay direction.

The normalized DAS are shown in Figure 4c,d for TMP. These DAS are compared to scaled lineouts at +400 fs in the case of the 4.95 eV pump and ±400 fs in the case of the 5.17 eV pump. These lineouts are chosen as they are representative of the VDEs of the states from which relaxation is occurring as they lie significantly outside of the IRF, but still within the lifetime of the state. Since the DAS match well with the lineouts, the GLA routine accurately fits the decay components in both directions.

GLA was used to extract fitted lifetimes which are shown in Table 1 for T, Thd, and TMP. For each kinetic component,

Table 1. Fitted Lifetimes of DAS_A (Tunable UV Pump) and DAS_B (6.20 eV Pump) for T, Thd, and TMP with Energies Ranging from 4.74 to 6.20 eV[a]

		τ (fs)		
pump (eV)	probe (eV)	T	Thd	TMP
4.74	6.20	360^{+60}_{-60}	390^{+70}_{-60}	870^{+180}_{-130}
4.95	6.20	390^{+60}_{-70}	410^{+70}_{-110}	840^{+60}_{-190}
5.17	6.20	410^{+140}_{-20}	430^{+20}_{-130}	610^{+140}_{-50}
6.20	5.17	650^{+470}_{-300}	590^{+260}_{-390}	550^{+290}_{-100}

[a]Note that the lifetime in the experiments with a 6.20 eV pump and 4.74 and 4.95 eV probes was unable to be fit and was not included in this table. The error bars presented represent the 95% confidence interval.

the functional form used was a single exponential decay convolved with a Gaussian IRF and a Heaviside function. The form of this expression is shown in the Supporting Information (Equation S1). Error bars were generated with the use of a support plane analysis and are reported at the 95% confidence interval.

QM/MM CASSCF calculations in solution (see Figure S5 in the Supporting Information) of the vertical excitation energies of the two lowest lying excited states show that the nature of the first excited state is nπ^*, with an oscillator strength close to zero. The lowest bright state is the second excited state, featuring a $\pi\pi^*$ character. At the CASSCF level, the energy difference between these two states is quite large: 2.04 eV for T, 1.88 eV for Thd, and 1.90 eV for TMP. After including dynamic correlation with XMS-CASPT2 (see Figure 5), the

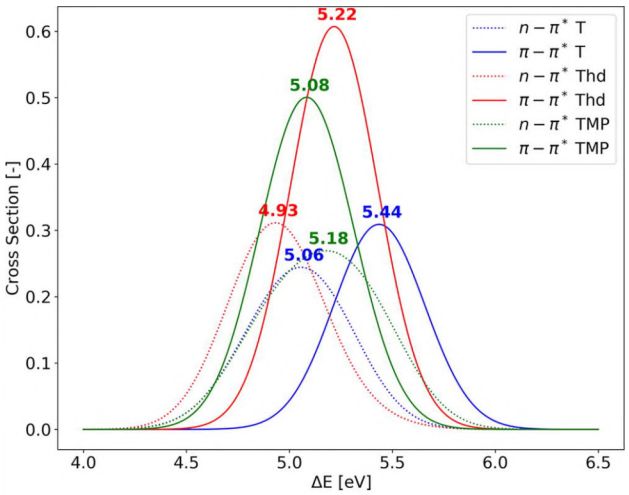

Figure 5. Absorption spectra of T (in blue), Thd (in red), and $TMP^{(-1)}$ (in green) calculated using QM/MM with XMS-CASPT2-(8/7)/6-31G*. The spectra were obtained through the procedure described in the Supporting Information; since the nπ^* oscillator strength is close to zero, it has been multiplied by 500 in order to compare the two excited state energies (the predicted absorption spectrum would consist only of the solid lines). The experimental absorption maxima are 4.68 eV for both T and Thd, compared to 5.02 and 5.08 eV from the calculations, respectively.

nπ^* and $\pi\pi^*$ states become near-degenerate. The average nπ^*/$\pi\pi^*$ energy difference is found to be 0.46 eV in T and 0.28 eV in Thd, but the two states get so close in TMP that we observe a swap in ~55% of the cases, and the average nπ^*/$\pi\pi^*$ energy difference falls to 0.15 eV.

DISCUSSION

Relaxation from the $\pi\pi^*$ State. The first $\pi\pi^*$ state is accessed through direct absorption by the tunable-UV pulses used in this experiment (4.74−5.17 eV) and decays within ~400 fs for both T and Thd while showing no pump energy dependence and almost no difference between the two molecules. We can directly compare our 4.74/6.20 eV experiments to those of Lübcke and co-workers at 4.66/5.21 eV.[34] Our lifetimes of 360^{+60}_{-60} and 390^{+70}_{-60} fs for T and Thd, respectively, are within error of the previous lifetimes of 410 ± 80 and 390 ± 20 fs. Note that the error bars here have been extended to the 95% confidence interval for Lübcke's work for a direct comparison. Extending the probe photon energy from the previous TRPES study clarifies that the measured time constants in that work were not limited by the accessibility of the Franck−Condon window; otherwise we would observe a longer $\pi\pi^*$ lifetime at our higher probe photon energy. Interestingly, the lifetimes in both TRPES experiments are somewhat shorter than those measured by TA (540 ± 40 fs)[29] or FU (470 ± 10 or 633 ± 18 fs).[28,51]

Although the lifetimes in T and Thd reported here appear to increase as the pump energy is raised, these differences are not significant in light of the error bars. A similar situation was seen in liquid jet studies of adenosine (Ado), where there was a slight decrease in lifetime with increasing pump energy that was also within error bars.[36,38] However, what does differ from adenine and its derivatives are the lifetimes themselves, which are notably longer for T (Thd) than for A (Ado): ~360 (390) fs compared to ~200 (250) fs.[29,36,38,52−54] This difference may arise simply from a flatter reaction coordinate leading to the CI for the thymine compounds, or from differing dynamics at the relevant CIs.

Despite the similarities in the absorption spectra of the three molecules, relaxation from the $\pi\pi^*$ state is quite different in TMP than in T and Thd. We find that TMP shows $\pi\pi^*$ lifetimes between 610 and 870 fs compared to ~400 fs in T and Thd. Moreover, the TMP lifetime drops considerably (from 840 to 610 fs) when the pump energy is increased from 4.95 to 5.17 eV. Our values are close to those of Onidas et al.,[28] who measured lifetimes of 680 ± 20 fs for TMP and 470 ± 10 fs for Thd at pump energies of 4.64 and 4.59 eV, respectively. Peon et al.[27] found lifetimes of 980 ± 120 fs for TMP and 700 ± 120 fs for Thd, although it is worth noting that all of their measured lifetimes are systematically longer than more recent measurements.[28,30−34] Nonetheless, the trend that TMP has a longer lifetime than T or Thd seems consistent across several experiments.

Indeed, the differences between molecules observed from the analysis of the computed absorption spectrum are too small to justify a remarkably longer excited state lifetime for TMP, especially since the absorption spectra of Thd and TMP are very similar. However, a closer inspection of the molecular conformation along the MM trajectories (using clustering analysis as described in the Supporting Information) reveals a different behavior for Thd and TMP. Two main conformations exist for Thd, which differ in the orientation between the thymine and deoxyribose rings: the molecule spends ~70% of the time in a conformation featuring the $O_5'-H_{O_5'}$ bond pointing toward O_2 (*syn* conformation, see **1a** in Figure 6; for the full atom nomenclature, see Figure S8 in the Supporting Information), while an ~180° rotation around the bond connecting the two rings leads to the conformation that is occupied for the remaining time (*anti* conformation, **1b** in Figure 6). The ground state energy difference between the two conformations, according to PBE0/6-31G* calculations using PCM,[55] is 2 kcal/mol, with **1a** being more stable than **1b**, independent of the solvent dielectric constant (see the Supporting Information for details). The dominance of **1a** was also seen in theoretical work by Pepino et al.[11] and is explained by the existence in the *syn* conformation of the aforementioned hydrogen bond between $O_5'-H_{O_5'}$ and O_2.

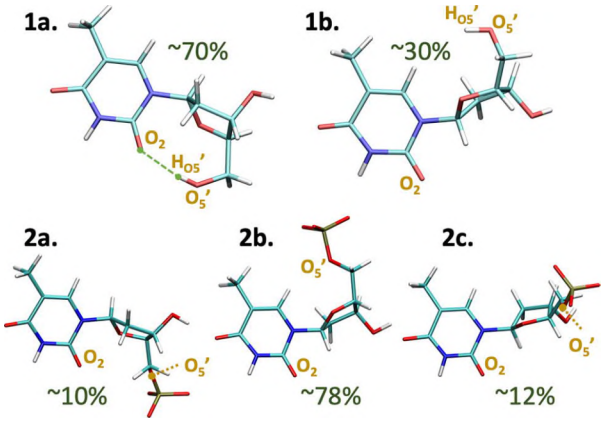

Figure 6. Main conformations of Thd (**1a** and **1b**) and TMP (**2a**, **2b**, and **2c**) along a 100 ns MM trajectory, with the corresponding percentage of occupation.

Due to the replacement of the OH group with a phosphate group in TMP, the situation is reversed. The conformation analogous to **1a** (i.e., **2a**), now featuring no intramolecular hydrogen bonds, is occupied only ~10% of the time, while the large majority of the trajectory is spent in conformations similar to **1b** and differentiated only by the orientation of the phosphate group with respect to the thymine ring (**2b** and **2c**). Indeed, **2c** does not correspond to a local minimum on the ground state potential energy surface: optimizing this geometry leads to **2b**, i.e., the *anti* conformation. At the PBE0/6-31G* level of theory, **2b** is ~7 kcal/mol more stable than **2a** (see the Supporting Information); these energy results are in agreement with the relative population of the respective conformations obtained from empirical force field based molecular dynamics, both for Thd and for TMP. The energy difference between conformations **2a** and **2b** increases in an apolar solvent, due to the net charge of the molecule.

These conformational transitions are unlikely to be of relevance in the excited state dynamics, since the simulated time scale of *syn*−*anti* conversion is in the tens-of-picoseconds range for both Thd and TMP (see Table S2 for details). This isomerization time scale is much longer than the excited state lifetime for both molecules. Since the isomerization time scales are derived from ground state dynamics, conformational transitions in the excited state dynamics cannot be completely excluded. Nevertheless, we find this possibility unlikely and suggest that any influence of the different conformations is restricted to the dependence of the ensuing excited state dynamics on the initial geometry (*syn* vs *anti*). This deserves further exploration, and future studies will concentrate on the influence of the starting conformation on photoexcitation dynamics. We expect that the classical description of intramolecular and solvent−solute hydrogen bonding should be accurate in our simulations, as the employed force field has

been chosen for its capacity to optimally describe thermodynamic, structural, and kinetic bulk properties introducing flexibility in the water molecule.[56]

The longer-time dynamics of TMP, displayed in Figure 3 for a pump photon energy of 4.95 eV, show that the signal decays substantially in the positive direction and, by 4 ps, all of the signal is gone. This result is also seen for T and Thd, as shown in Figures S2 and S3. The absence of signal beyond 4 ps is of interest in light of previous work based on TA that found a decay component that persists on the order of tens of picoseconds in addition to the subpicosecond decay.[29−32] This long-lived signal has been attributed to trapping in an intermediate $n\pi^*$ state before reaching S_0. As previously mentioned, long-lived signal was also not seen in the previous liquid jet TRPES study on T and Thd;[34] based on calculations indicating that ionization from the $n\pi^*$ state would be accessible at the highest probe energy (5.20 eV) used in that work, the authors concluded that the $n\pi^*$ state did not participate in the dynamics.

Recent gas phase work using TRPES on thymine using an XUV probe at 14 eV has located the $n\pi^*$ state experimentally, showing a feature covering an electron binding energy range of 6−7 eV with a vertical ionization energy around 6.5 eV.[24] In water, one expects these values to decrease by about 1 eV owing to favorable hydration of the cation.[40] Under these circumstances, it is possible that the probe energy of 5.20 eV used previously was insufficient to ionize the $n\pi^*$ state (note that ionization from this state to the cation ground state is not possible via a one-electron transition), but the higher probe energy of 6.20 eV used here would certainly be sufficient. Hence there is no evidence for a long-lived $n\pi^*$ in our work, either. It is possible that the photoionization cross section of the $n\pi^*$ state is very small, in which case no signal would be seen from this state in our experiment.

While earlier TA studies[30−32] were fairly confident in their assignment of the $n\pi^*$ state as the reason for a multiple picoseconds signal, a recent experiment[33] instead proposed two long-lived states; a $^3\pi\pi^*$ state and a state of unknown character. The energetics of this triplet state in liquid water have been considered by Pepino et al.[17] They predict the binding energy of the $^3\pi\pi^*$ state to be 5.6 eV, which would enable ionization by our probe laser, but produce low energy (0.6 eV) photoelectrons that are near the lower limit of our detection efficiency. Also, in this same paper, the $^3\pi\pi^*$ state is calculated to lie ∼1.3 eV below the $n\pi^*$ state, which would put it out of range of our probe laser based on the estimate of the $n\pi^*$ ionization energy given above. Hence, it is possible that the $^3\pi\pi^*$ state is involved in the overall mechanism but cannot be seen in our experiment. The possible role of the intermediate electronic states in the relaxation of thymine will be explored in planned experiments using higher probe photon energies.

The role of the $n\pi^*$ state in nucleobase relaxation is crucial to understanding DNA damage as this state has been implicated in the formation of unwanted photoproducts and as an intermediate in the formation of the $^3\pi\pi^*$ state.[57] For example, one of the most prominent pathways of DNA damage, thymine dimerization, occurs when covalent bonds are formed between adjacent thymine nucleobases in DNA strands, most commonly as cyclobutane pyrimidine dimers or 6−4 photoproducts which are both likely formed through a long-lived intermediate state.[1,30] Because these long-lived excited states are not observed here in the relaxation of single subunits of T, Thd, or TMP, this excited state trapping process may likely be the result of or enhanced by interaction between bases. This result specifically warrants the study of the TpT dinucleotide, and such studies are planned in the near future.

Relaxation from S_n. Using pump photons at 6.20 eV, the higher lying electronic band of T and its derivatives was populated. Multiple overlapping $\pi\pi^*$ transitions are predicted to contribute to this band,[11] and no dynamical studies resulting from its excitation have been carried out prior to this work. Relaxation from this higher lying band is shown in the negative delay direction in all data sets, but can only be fit in the case of the 5.17 eV probe photon energy for all three molecules. As can be seen in comparing Figures 1 and 2, the signal in the negative direction is more intense and persists for longer delays. This likely indicates that probe photon energies below 5.17 eV do not yield sufficiently high eKE for S_n dynamics to be reliably characterized; due to the transformation from ToF to eKE, features below ∼0.5 eV can be quite noisy and hard to fit. In our previous study of Ado and adenosine monophosphate (AMP), relaxation from S_n was seen only for AMP.[38] However, the highest probe energy used in that work was 4.97 eV, the probe energy corresponding to Figure 1 in this work.

For T, Thd, and TMP, decay of the S_n signal occurs in ∼600 fs. The decay of S_n for T and Thd appears to be longer than the decay of the lower lying $\pi\pi^*$ state (∼400 fs vs ∼600 fs) although the error bars for the S_n lifetimes are large. A similar trend was seen in AMP.[38] In all cases, the VDEs of the state observed by pumping either the S_n band or the lower $\pi\pi^*$ state are similar, which suggests that excitation at 6.20 eV promotes electrons to S_n, followed by relaxation into the lower lying $\pi\pi^*$ state within the IRF of the pulses used. Photoionization then occurs from the lower lying $\pi\pi^*$ surface. The absence of photoionization signal from the upper band may reflect a lower ionization cross section and/or an extremely short lifetime, as has been observed in other highly excited $\pi\pi^*$ states in TRPES.[58]

Signal from upper band excitation is notably stronger from TMP than from T and Thd, although its lifetime is within error of that from T and Thd. Hence, the relaxation pathway is likely to be similar, but the origin of the stronger upper band signal for TMP (and for AMP) requires additional investigation.

■ CONCLUSIONS

The relaxation dynamics of thymine (T) and its derivatives thymidine (Thd) and thymidine monophosphate (TMP) were studied using time-resolved photoelectron spectroscopy on a water microjet. Two states are directly populated by ultraviolet absorption in the range 4.74−6.20 eV. As confirmed by XMS-CASPT2//CASSCF/AMBER calculations, the first absorption band is populated using light in the range 4.74−5.17 eV, which corresponds to the lowest lying bright state of $\pi\pi^*$ character, while the 6.20 eV light populates a higher lying band which contains multiple states of $\pi\pi^*$ character. Relaxation from the lower lying $\pi\pi^*$ state occurs in ∼400 fs for both T and Thd and ∼670−840 fs in TMP, in general agreement with previous studies. The computational analysis suggests that this difference is linked to conformational differences existing between Thd and TMP, which might influence the topology of the excited state potential energy surface. Notably, no long-lived signal was seen to persist past ∼1.5 ps, indicating that the $n\pi^*$ does not participate in the relaxation process. Excitation to the S_n band appears to result in rapid decay to the lower lying $\pi\pi^*$

state within the duration of the pulses used in the experiment and then back into the ground state.

AUTHOR INFORMATION

ORCID

Blake A. Erickson: 0000-0002-0763-890X
Zachary N. Heim: 0000-0002-0240-7096
Elisa Pieri: 0000-0002-5377-5382
Erica Liu: 0000-0002-1193-0049
Todd J. Martinez: 0000-0002-4798-8947
Daniel M. Neumark: 0000-0002-3762-9473

Notes

The authors declare no competing financial interest.

ACKNOWLEDGMENTS

The experimental work was funded by the National Science Foundation under Grant No. CHE-1663832. Additional support was provided by the Air Force Office of Scientific Research as part of a Multidisciplinary University Initiative, MURI, under Award No. 24086151-01 and the University of California at Berkeley Center for Solvation Studies, CALSOLV. Z.N.H. is supported through the University of California at Berkeley Department of Chemistry Graduate Student Fellowship Support. T.J.M and E.P. were supported by the AMOS program within the Chemical Sciences, Geosciences and Biosciences Division of the Office of Basic Energy Sciences, Office of Science, U.S. Department of Energy. The data presented here are available on request sent to dneumark@berkeley.edu.

REFERENCES

(1) Crespo-Hernández, C. E.; Cohen, B.; Hare, P. M.; Kohler, B. Ultrafast Excited-State Dynamics in Nucleic Acids. *Chem. Rev.* **2004**, *104*, 1977−2019.

(2) Shukla, M. K.; Leszczynski, J. Electronic Spectra, Excited State Structures and Interactions of Nucleic Acid Bases and Base Assemblies: A Review. *J. Biomol. Struct. Dyn.* **2007**, *25*, 93−118.

(3) Middleton, C. T.; de La Harpe, K.; Su, C.; Law, Y. K.; Crespo-Hernández, C. E.; Kohler, B. DNA Excited-Etate Dynamics: From Single Bases to the Double Helix. *Annu. Rev. Phys. Chem.* **2009**, *60*, 217−239.

(4) Barbatti, M. *Photoinduced Phenomena in Nucleic Acids I*; Springer: 2015; Vol. 355.

(5) Improta, R.; Santoro, F.; Blancafort, L. Quantum Mechanical Studies on the Photophysics and the Photochemistry of Nucleic Acids and Nucleobases. *Chem. Rev.* **2016**, *116*, 3540−3593.

(6) Stavros, V. G.; Verlet, J. R. R. Gas-Phase Femtosecond Particle Spectroscopy: A Bottom-Up Approach to Nucleotide Dynamics. *Annu. Rev. Phys. Chem.* **2016**, *67*, 211−232.

(7) Kleinermanns, K.; Nachtigallová, D.; de Vries, M. S. Excited State Dynamics of DNA Bases. *Int. Rev. Phys. Chem.* **2013**, *32*, 308−342.

(8) Kohler, B. Nonradiative Decay Mechanisms in DNA Model Systems. *J. Phys. Chem. Lett.* **2010**, *1*, 2047−2053.

(9) Fox, J. J.; Shugar, D. Spectrophotometric Studies on Nucleic Acid Derivatives and Related Compounds as a Function of PH. II. Natural and Synthetic Pyrimidine Nucleosides. *Biochim. Biophys. Acta* **1952**, *9*, 369−384.

(10) Wilson, W. 229. Some 2:4-Diamino-5-Acylamido-6-Hydroxypyrimidines. *J. Chem. Soc.* **1948**, 1157−1161.

(11) Pepino, A. J.; Segarra-Martí, J.; Nenov, A.; Improta, R.; Garavelli, M. Resolving Ultrafast Photoinduced Deactivations in Water-Solvated Pyrimidine Nucleosides. *J. Phys. Chem. Lett.* **2017**, *8*, 1777−1783.

(12) Voet, D.; Gratzer, W. B.; Cox, R. A.; Doty, P. Absorption Spectra of Nucleotides, Polynucleotides, and Nucleic Acids in the Far Ultraviolet. *Biopolymers* **1963**, *1*, 193−208.

(13) Schreiber, M.; Silva-Junior, M. R.; Sauer, S. P. A.; Thiel, W. Benchmarks for Electronically Excited States: CASPT2, CC2, CCSD, and CC3. *J. Chem. Phys.* **2008**, *128*, 134110.

(14) Zechmann, G.; Barbatti, M. Photophysics and Deactivation Pathways of Thymine. *J. Phys. Chem. A* **2008**, *112*, 8273−8279.

(15) Barbatti, M.; Aquino, A. J. A.; Lischka, H. The UV Absorption of Nucleobases: Semi-Classical Ab Initio Spectra Simulations. *Phys. Chem. Chem. Phys.* **2010**, *12*, 4959.

(16) Szalay, P. G.; Watson, T.; Perera, A.; Lotrich, V. F.; Bartlett, R. J. Benchmark Studies on the Building Blocks of DNA. 1. Superiority of Coupled Cluster Methods in Describing the Excited States of Nucleobases in the Franck-Condon Region. *J. Phys. Chem. A* **2012**, *116*, 6702−6710.

(17) Pepino, A. J.; Segarra-Martí, J.; Nenov, A.; Rivalta, I.; Improta, R.; Garavelli, M. UV-Induced Long-Lived Decays in Solvated Pyrimidine Nucleosides Resolved at the MS-CASPT2/MM Level. *Phys. Chem. Chem. Phys.* **2018**, *20*, 6877−6890.

(18) Kang, H.; Lee, K. T.; Jung, B.; Ko, Y. J.; Kim, S. K. Intrinsic Lifetimes of the Excited State of DNA and RNA Bases. *J. Am. Chem. Soc.* **2002**, *124*, 12958−12959.

(19) He, Y.; Wu, C.; Kong, W. Decay Pathways of Thymine and Methyl-Substituted Uracil and Thymine in the Gas Phase. *J. Phys. Chem. A* **2003**, *107*, 5145−5148.

(20) Canuel, C.; Mons, M.; Piuzzi, F.; Tardivel, B.; Dimicoli, I.; Elhanine, M. Excited States Dynamics of DNA and RNA Bases: Characterization of a Stepwise Deactivation Pathway in the Gas Phase. *J. Chem. Phys.* **2005**, *122*, 074316.

(21) Ullrich, S.; Schultz, T.; Zgierski, M. Z.; Stolow, A. Electronic Relaxation Dynamics in DNA and RNA Bases Studied by Time-Resolved Photoelectron Spectroscopy. *Phys. Chem. Chem. Phys.* **2004**, *6*, 2796−2801.

(22) Hudock, H. R.; Levine, B. G.; Thompson, A. L.; Satzger, H.; Townsend, D.; Gador, N.; Ullrich, S.; Stolow, A.; Martínez, T. J. Ab Initio Molecular Dynamics and Time-Resolved Photoelectron Spectroscopy of Electronically Excited Uracil and Thymine. *J. Phys. Chem. A* **2007**, *111*, 8500−8508.

(23) Wolf, T. J. A.; Myhre, R. H.; Cryan, J. P.; Coriani, S.; Squibb, R. J.; Battistoni, A.; Berrah, N.; Bostedt, C.; Bucksbaum, P.; Coslovich, G. Probing Ultrafast $\pi\pi^*/n\pi^*$ Internal Conversion in Organic Chromophores via K-Edge Resonant Absorption. *Nat. Commun.* **2017**, *8*, 29.

(24) Wolf, T. J. A.; Parrish, R. M.; Myhre, R. H.; Martínez, T. J.; Koch, H.; Gühr, M. Observation of Ultrafast Intersystem Crossing in Thymine by Extreme Ultraviolet Time-Resolved Photoelectron Spectroscopy. *J. Phys. Chem. A* **2019**, *123*, 6897−6903.

(25) Barbatti, M.; Aquino, A. J. A.; Szymczak, J. J.; Nachtigallová, D.; Hobza, P.; Lischka, H. Relaxation Mechanisms of UV-Photoexcited DNA and RNA Nucleobases. *Proc. Natl. Acad. Sci. U. S. A.* **2010**, *107*, 21453−21458.

(26) Picconi, D.; Lami, A.; Santoro, F. Hierarchical Transformation of Hamiltonians with Linear and Quadratic Couplings for Non-

adiabatic Quantum Dynamics: Application to the $\pi\pi^*/n\pi^*$ Internal Conversion in Thymine. *J. Chem. Phys.* **2012**, *136*, 244104.
(27) Peon, J.; Zewail, A. H. DNA/RNA Nucleotides and Nucleosides: Direct Measurement of Excited-State Lifetimes by Femtosecond Fluorescence Up-Conversion. *Chem. Phys. Lett.* **2001**, *348*, 255−262.
(28) Onidas, D.; Markovitsi, D.; Marguet, S.; Sharonov, A.; Gustavsson, T. Fluorescence Properties of DNA Nucleosides and Nucleotides: A Refined Steady-State and Femtosecond Investigation. *J. Phys. Chem. B* **2002**, *106*, 11367−11374.
(29) Pecourt, J. M. L.; Peon, J.; Kohler, B. DNA Excited-State Dynamics: Ultrafast Internal Conversion and Vibrational Cooling in a Series of Nucleosides. *J. Am. Chem. Soc.* **2001**, *123*, 10370−10378.
(30) Hare, P. M.; Crespo-Hernández, C. E.; Kohler, B. Internal Conversion to the Electronic Ground State Occurs via Two Distinct Pathways for Pyrimidine Bases in Aqueous Solution. *Proc. Natl. Acad. Sci. U. S. A.* **2007**, *104*, 435−440.
(31) Xue, B.; Yabushita, A.; Kobayashi, T. Ultrafast Dynamics of Uracil and Thymine Studied Using a Sub-10 fs Deep Ultraviolet Laser. *Phys. Chem. Chem. Phys.* **2016**, *18*, 17044−17053.
(32) Prokhorenko, V. I.; Picchiotti, A.; Pola, M.; Dijkstra, A. G.; Miller, R. J. D. New Insights into the Photophysics of DNA Nucleobases. *J. Phys. Chem. Lett.* **2016**, *7*, 4445−4450.
(33) Pilles, B. M.; Maerz, B.; Chen, J.; Bucher, D. B.; Gilch, P.; Kohler, B.; Zinth, W.; Fingerhut, B. P.; Schreier, W. J. Decay Pathways of Thymine Revisited. *J. Phys. Chem. A* **2018**, *122*, 4819−4828.
(34) Buchner, F.; Nakayama, A.; Yamazaki, S.; Ritze, H. H.; Lübcke, A. Excited-State Relaxation of Hydrated Thymine and Thymidine Measured by Liquid-Jet Photoelectron Spectroscopy: Experiment and Simulation. *J. Am. Chem. Soc.* **2015**, *137*, 2931−2938.
(35) Cerezo, J.; Liu, Y.; Lin, N.; Zhao, X.; Improta, R.; Santoro, F. Mixed Quantum/Classical Method for Nonadiabatic Quantum Dynamics in Explicit Solvent Models: The $\pi\pi^*/n\pi^*$ Decay of Thymine in Water as a Test Case. *J. Chem. Theory Comput.* **2018**, *14*, 820−832.
(36) Buchner, F.; Ritze, H. H.; Lahl, J.; Lübcke, A. Time-Resolved Photoelectron Spectroscopy of Adenine and Adenosine in Aqueous Solution. *Phys. Chem. Chem. Phys.* **2013**, *15*, 11402−11408.
(37) Buchner, F.; Heggen, B.; Ritze, H.-H.; Thiel, W.; Lübcke, A. Excited-State Dynamics of Guanosine in Aqueous Solution Revealed by Time-Resolved Photoelectron Spectroscopy: Experiment and Theory. *Phys. Chem. Chem. Phys.* **2015**, *17*, 31978−31987.
(38) Williams, H. L.; Erickson, B. A.; Neumark, D. M. Time-Resolved Photoelectron Spectroscopy of Adenosine and Adenosine Monophosphate Photodeactivation Dynamics in Water Microjets. *J. Chem. Phys.* **2018**, *148*, 194303.
(39) Winter, B.; Faubel, M. Photoemission from Liquid Aqueous Solutions. *Chem. Rev.* **2006**, *106*, 1176−1211.
(40) Seidel, R.; Winter, B.; Bradforth, S. E. Valence Electronic Structure of Aqueous Solutions: Insights from Photoelectron Spectroscopy. *Annu. Rev. Phys. Chem.* **2016**, *67*, 283−305.
(41) Suzuki, T. Time-Resolved Photoelectron Spectroscopy of Non-Adiabatic Electronic Dynamics in Gas and Liquid Phases. *Int. Rev. Phys. Chem.* **2012**, *31*, 265−318.
(42) Faubel, M.; Siefermann, K. R.; Liu, Y.; Abel, B. Ultrafast Soft X-Ray Photoelectron Spectroscopy at Liquid Water Microjets. *Acc. Chem. Res.* **2012**, *45*, 120−130.
(43) Shreve, A. T.; Yen, T. A.; Neumark, D. M. Photoelectron Spectroscopy of Hydrated Electrons. *Chem. Phys. Lett.* **2010**, *493*, 216−219.
(44) Shreve, A. T.; Elkins, M. H.; Neumark, D. M. Photoelectron Spectroscopy of Solvated Electrons in Alcohol and Acetonitrile Microjets. *Chem. Sci.* **2013**, *4*, 1633−1639.
(45) Elkins, M. H.; Williams, H. L.; Shreve, A. T.; Neumark, D. M. Relaxation Mechanism of the Hydrated Electron. *Science* **2013**, *342*, 1496−1499.
(46) Elkins, M. H.; Williams, H. L.; Neumark, D. M. Dynamics of Electron Solvation in Methanol: Excited State Relaxation and Generation by Charge-Transfer-to-Solvent. *J. Chem. Phys.* **2015**, *142*, 234501.
(47) Elkins, M. H.; Williams, H. L.; Neumark, D. M. Isotope Effect on Hydrated Electron Relaxation Dynamics Studied with Time-Resolved Liquid Jet Photoelectron Spectroscopy. *J. Chem. Phys.* **2016**, *144*, 184503.
(48) Faubel, M.; Schlemmer, S.; Toennies, J. P. A Molecular Beam Study of the Evaporation of Water from a Liquid Jet. *Z. Phys. D: At., Mol. Clusters* **1988**, *10*, 269−277.
(49) Knutson, J. R.; Davenport, L.; Brand, L. Anisotropy Decay Associated Fluorescence Spectra and Analysis of Rotational Heterogeneity. 1. Theory and Applications. *Biochemistry* **1986**, *25*, 1805−1810.
(50) Van Stokkum, I. H. M.; Larsen, D. S.; Van Grondelle, R. Global and Target Analysis of Time-Resolved Spectra. *Biochim. Biophys. Acta, Bioenerg.* **2004**, *1657*, 82−104.
(51) Gustavsson, T.; Bányász, Á.; Lazzarotto, E.; Markovitsi, D.; Scalmani, G.; Frisch, M. J.; Barone, V.; Improta, R. Singlet Excited-State Behavior of Uracil and Thymine in Aqueous Solution: A Combined Experimental and Computational Study of 11 Uracil Derivatives. *J. Am. Chem. Soc.* **2006**, *128*, 607−619.
(52) Pecourt, J. M. L.; Peon, J.; Kohler, B. Ultrafast Internal Conversion of Electronically Excited RNA and DNA Nucleosides in Water. *J. Am. Chem. Soc.* **2000**, *122*, 9348−9349.
(53) Gustavsson, T.; Sharonov, A.; Onidas, D.; Markovitsi, D. Adenine, Deoxyadenosine and Deoxyadenosine 5′-Monophosphate Studied by Femtosecond Fluorescence Upconversion Spectroscopy. *Chem. Phys. Lett.* **2002**, *356*, 49−54.
(54) Gustavsson, T.; Sarkar, N.; Vayá, I.; Jiménez, M. C.; Markovitsi, D.; Improta, R. A Joint Experimental/Theoretical Study of the Ultrafast Excited State Deactivation of Deoxyadenosine and 9-Methyladenine in Water and Acetonitrile. *Photochem. Photobiol. Sci.* **2013**, *12*, 1375−1386.
(55) Tomasi, J.; Mennucci, B.; Cammi, R. Quantum Mechanical Continuum Solvation Models. *Chem. Rev.* **2005**, *105*, 2999−3093.
(56) Wu, Y.; Tepper, H. L.; Voth, G. A. Flexible Simple Point-Charge Water Model with Improved Liquid-State Properties. *J. Chem. Phys.* **2006**, *124*, 024503.
(57) Cadet, J. *Bioorganic Photochemistry*; Morrison, H., Ed.; John Wiley & Sons, Ltd.: 1990.
(58) Horio, T.; Spesyvtsev, R.; Nagashima, K.; Ingle, R. A.; Suzuki, Y.; Suzuki, T. Full Observation of Ultrafast Cascaded Radiationless Transitions from S_2 ($\pi\pi^*$) State of Pyrazine Using Vacuum Ultraviolet Photoelectron Imaging. *J. Chem. Phys.* **2016**, *145*, 044306.